### Title
Inhalation intake fraction of particulate matter from localized indoor emissions




### Authors
Licina, Dusan
Tian, Yilin
Nazaroff, William W



### Publication Date
2017-10-01

### DOI
10.1016/j.buildenv.2017.06.037

Peer reviewed

Elsevier Editorial System(tm) for Building and Environment

Manuscript Draft

Manuscript Number:

Title: Inhalation intake fraction of particulate matter from localized indoor emissions

Article Type: Original Research Paper

Keywords: Inhalation intake, Indoor particles, Source location, Exposure duration, Thermal plume, Human activity.

Corresponding Author: Dr. Dusan Licina, PhD

Corresponding Author's Institution: University of California Berkeley

First Author: Dusan Licina, PhD

Order of Authors: Dusan Licina, PhD; Yilin Tian; William W Nazaroff

Abstract: Elevated exposure to airborne particulate matter is linked to deleterious health and well-being outcomes. Exposure assessment can be improved through enhanced understanding of source-receptor relationships, for example as expressed in the inhalation intake fraction metric. This study provides new knowledge about how inhalation intake of airborne particles varies with spatially varying indoor emissions. In a controlled environmental chamber with low background particle levels, we monitored the time- and size-resolved particle concentrations at multiple locations including the subject's breathing zone. We investigated two types of particle emissions: (i) controlled releases from several specific indoor locations; and (ii) natural release from skin and clothing for a range of simulated occupant activities. Findings show that particles released proximate to the human envelope caused 7-10 per thousand total inhalation intake fraction, which was 1.5-16x higher than the intake fraction for other indoor release locations. These outcomes reflect the influence of emissions-receptor proximity combined with the efficient transport of particles by means of the thermal plume to the breathing zone. The results show that the well-mixed representation of an indoor environment could underestimate the inhalation intake by 40-90% for various localized indoor emissions, and by up to 3x for particles emitted from the human envelope. The post-release exposure period contributed substantially to total inhalation intake. For particles released naturally from the human envelope, inhalation intake fractions varied with activity type and were higher for a subject when seated rather than walking.

Suggested Reviewers: Viviana Acevedo-Bolton
Department of Civil and Environmental Engineering, Stanford University
vivianaa@stanford.edu

Atila Novoselac
Department of Civil, Architectural, and Environmental Engineering, University of Texas at Austin
atila@mail.utexas.edu

Alvin Lai

Associate Professor, Department of Building and Construction, City University of Hong Kong
alvinlai@cityu.edu.hk

23 March 2017

Professor Qingyan Chen
Editor-in-Chief, *Building and Environment*

Dear Professor Chen,

On behalf of the authors, I am pleased to submit a research manuscript to be considered for publication in *Building and Environment*:

**Inhalation intake fraction of particulate matter from localized indoor emissions**

Dusan Licina, Yilin Tian and William W Nazaroff

In this manuscript, we present an experimental investigation of the inhalation intake of airborne particles associated with spatially varying indoor emissions. Previous studies have reported inhalation intake fractions associated with indoor particle sources, and most of these have relied on mathematical modelling approaches and well-mixed representation of indoor spaces. A key aspect when considering localized indoor releases of particulate matter is that the spatial distribution of indoor pollution is sometimes not well represented by the common approximation of perfectly mixed indoor air. Our study adds to previous work by deepening our understanding of the inhalation intake fraction metric in relation to different types of localized particle-phase indoor pollutants, their spatiotemporal variability, and the influential transport mechanisms. In this study, we combine the empirical data from deliberately released localized particle sources with results inferred from measurements of exposure to particle releases from the human envelope, including skin and clothing. This research contributes to an improved understanding of the inhalation intake fraction by elucidating source-receptor relationships. The findings could be beneficial for interpreting the health risks associated with indoor sources, for improving accuracy in exposure assessment, and for developing improved exposure control strategies.

The data set reported in this manuscript has not been previously published and is not under consideration for reporting in the same or substantially similar form in any other journal. All those listed as authors are qualified for authorship and all who are qualified to be authors are listed as authors on the byline.

To the author's knowledge, no conflict of interest, financial or otherwise, exists. Each author has participated and contributed sufficiently to take public responsibility for appropriate portions of the content. Thank you for your consideration of this manuscript.

Sincerely,

Dusan Licina (corresponding author)
Department of Civil and Environmental Engineering
University of California, Berkeley
624 Davis Hall, Berkeley, CA 94720-1710, USA
Phone: (925) 246-3654
E-mail: licinadusan@yahoo.com

## Highlights

- We study how intake fraction (iF) of airborne particles varies with spatially varying indoor emissions.
- Source position, thermal plume, and exposure duration considerably influence inhalation iF.
- Releases near the human cause much higher inhalation iF compared to other indoor release locations.
- Inhalation iF while walking was considerably lower than iF of a seated person.
- Well-mixed assumption could underestimate inhalation iF for certain indoor pollutant releases.

# Inhalation intake fraction of particulate matter from localized indoor emissions

Dusan Licina*, Yilin Tian, William W Nazaroff

Department of Civil and Environmental Engineering, University of California, Berkeley, California, United States of America

*Corresponding email: licinadusan@yahoo.com

## Abstract

Elevated exposure to airborne particulate matter is linked to deleterious health and well-being outcomes. Exposure assessment can be improved through enhanced understanding of source-receptor relationships, for example as expressed in the inhalation intake fraction metric. This study provides new knowledge about how inhalation intake of airborne particles varies with spatially varying indoor emissions. In a controlled environmental chamber with low background particle levels, we monitored the time- and size-resolved particle concentrations at multiple locations including the subject's breathing zone. We investigated two types of particle emissions: (i) controlled releases from several specific indoor locations; and (ii) natural release from skin and clothing for a range of simulated occupant activities. Findings show that particles released proximate to the human envelope caused 7–10 per thousand total inhalation intake fraction, which was 1.5–16× higher than the intake fraction for other indoor release locations. These outcomes reflect the influence of emissions-receptor proximity combined with the efficient transport of particles by means of the thermal plume to the breathing zone. The results show that the well-mixed representation of an indoor environment could underestimate the inhalation intake by 40-90% for various localized indoor emissions, and by up to 3× for particles emitted from the human envelope. The post-release exposure period contributed substantially to total

inhalation intake. For particles released naturally from the human envelope, inhalation intake fractions varied with activity type and were higher for a subject when seated rather than walking.

*Keywords*: Inhalation intake, Indoor particles, Source location, Exposure duration, Thermal plume, Human activity.

## 1. Introduction

Elevated inhalation exposure to airborne particles is correlated with detrimental health and well-being outcomes. Accurate assessment, effective control and mitigation of exposure to airborne particulate matter (PM) require understanding of quantitative relationships between source emissions and human intake. Indoors, such relationships vary with building-related factors (e.g. ventilation rate, air distribution and room size) and human-related factors (e.g. occupancy, activity and inhalation rate), as well as with pollutant attributes (e.g. source strength, particle transport and transformation) [1]. One metric that incorporates information about all of the important attributes influencing the source-receptor pathway is the inhalation intake fraction. This measure can be defined as the inhaled pollutant mass per unit mass released from a source [2]. Among other important features, the inhalation intake fraction highlights the importance of emissions from indoor sources contributing to exposure: the inhalation intake fraction for an indoor emission source can be 2-3 orders of magnitude higher than for an outdoor emission source [3-4].

Prominent sources of episodic indoor emissions of PM include smoking [5,6], cooking [7,8], cleaning [9,10] and resuspension [11,12]. Humans are significant contributors to indoor loads of coarse aerosol particles, owing in part to particle shedding from skin and clothing, particularly during vigorous activities [13-16]. Few studies have reported inhalation intake fractions associated with indoor particle sources, and most of these have relied on mathematical

modelling approaches. Lai et al. [4] calculated that inhalation intake fractions for emissions in buildings and moving vehicles vary in the range 1-100‰ (or 1000-100,000 parts per million, ppm). Values at the lower end of this range were determined in a simulation study of environmental tobacco smoke in residences [17], for dust particles released from blankets, pillows, and mattresses [18,19] and for droplets from simulated coughs [20].

A key aspect when considering localized indoor releases of PM is that the spatial distribution of indoor pollution is sometimes not well represented by the common approximation of perfectly mixed indoor air. In particular, for assessing short-term exposures and the resulting inhalation intake, spatial heterogeneity and finite mixing times play important roles [21-23]. Nazaroff [1] used a modeling approach to explore how the inhalation intake fraction was influenced by a combination of building factors, human attributes and pollutant related characteristics. Specific results in that study were based on the assumption of well-mixed indoor spaces. Further efforts are needed to deepen our understanding of the inhalation intake fraction metric in relation to different types of localized particle-phase indoor pollutants, their spatiotemporal variability, and the influential transport mechanisms.

The empirical study reported here investigates the inhalation intake fraction of PM from episodic, localized indoor emissions. By measuring the time- and size-resolved particle levels in the breathing zone, in the exhaust flow from the room, and at stationary locations within the room, we explore the influence of the location of indoor emissions, the spatiotemporal variability of PM concentrations, and some important transport processes. To assess the relative importance of source type, empirical data from deliberately released localized particle sources are combined with results inferred from measurements of exposure to particle releases from the human envelope, including skin and clothing. This research contributes to an improved understanding of

the inhalation intake fraction by elucidating source-receptor relationships. The findings could be beneficial for interpreting the health risks associated with indoor sources, for improving accuracy in exposure assessment, and for developing improved strategies for exposure control.

## 2. Methods

### *2.1. Study site and mechanical ventilation*

Experimental measurements were conducted in an environmental chamber with floor dimensions of 4.6 m × 4.6 m and an interior volume of ~ 50 $m^3$. The experimental chamber is situated within a larger thermally conditioned building, which provided protection from the influence of weather. The chamber is served by a dedicated heating, ventilating and air conditioning (HVAC) system that continuously supplies 100% outdoor air. The conditioned air is discharged into the chamber via two diffusers located at ceiling level and exhausted through a wall opening at 1.8 m height (Figure 1). During these experiments, the indoor dry-bulb temperature set point was 21 ± 1.5 °C, and the relative humidity was 40 ± 5%. Interior heat production from equipment and lighting summed to less than 100 W. The tracer gas decay method was applied using carbon dioxide to evaluate the air-exchange rate. The average value was 2.3 ± 0.05 $h^{-1}$ ($n$ = 5), corresponding to a volumetric flow rate of 115 $m^3$/h. Spot checks during the experiments confirmed that the ventilation rate was constant. Intrusion of PM from external sources into the experimental room was minimal because the supply air was provided through a particle filter with a manufacturer-specified efficiency of ≥ 95% for 0.3 μm particles. The only significant sources of PM were those deliberately generated indoors, as confirmed by measuring low background particle levels in the absence of indoor activities. The hard vinyl flooring of the chamber was suitable for limiting coarse particle resuspension to very low levels.

Prior to the start of experiments and at the end of each experimental day, the chamber flooring was thoroughly cleaned so as to further reduce uncontrolled resuspension from the floor.

### *2.2. Experimental design*

Basic experiments were designed to probe the influence of two types of particle emissions: controlled episodic sources released at various indoor locations; and emissions released naturally from the human envelope (skin and clothing).

For the controlled emissions, the receptor was a custom-built non-breathing thermal manikin. The manikin (Center for the Built Environment, UC Berkeley, CA) was dressed in long pants and a T-shirt, and was situated in the center of the room (Figure 1). The manikin has a complex male body shape, a height of 1.30 m in a seated posture (1.85 m when standing), and produces a sensible heat loss of 100 W, thus reasonably representing a human during sedentary office activities. Prior research has shown that the measurement and prediction of airflow characteristics in spaces occupied with sedentary people can be accurately performed with thermal manikins [24,25].

Deliberate releases occurred at nine indoor locations (Figure 1): proximate to manikin's groin (at 0.5 m height) to resemble particles released from the human body (experiment ID = 1); near the feet (at 0.1 m height) to represent particles detached from the shoes or from the floor owing to foot-floor contact by the subject (ID = 2); beneath the supply air diffuser (ID = 3, distance to diffuser 0.1 m) to mimic intrusion of particulate matter from the outdoor air through the ventilation duct; 1 m in front of the manikin at four heights (ID = 4 for height = 1.5 m; ID = 5, 1 m; ID = 6, 0.5 m; and ID = 7, 0.1 m) to simulate nearby indoor PM emission at various heights (e.g., another human body, cooking, smoking, resuspension from surfaces, etc.); and 2 m behind (ID = 8) and in front of the manikin (ID = 9) at 0.1 m height to represent particles

resuspended from flooring close to the seated subject. For each experiment, particles were released from one position at a constant rate for 10 minutes. Two supplementary experiments were designed to probe the influence of the thermal plume on the inhalation intake fraction. In these experiments, the manikin was not heated and particles were released proximate to the groin (ID = 10) and feet (ID = 11), respectively.

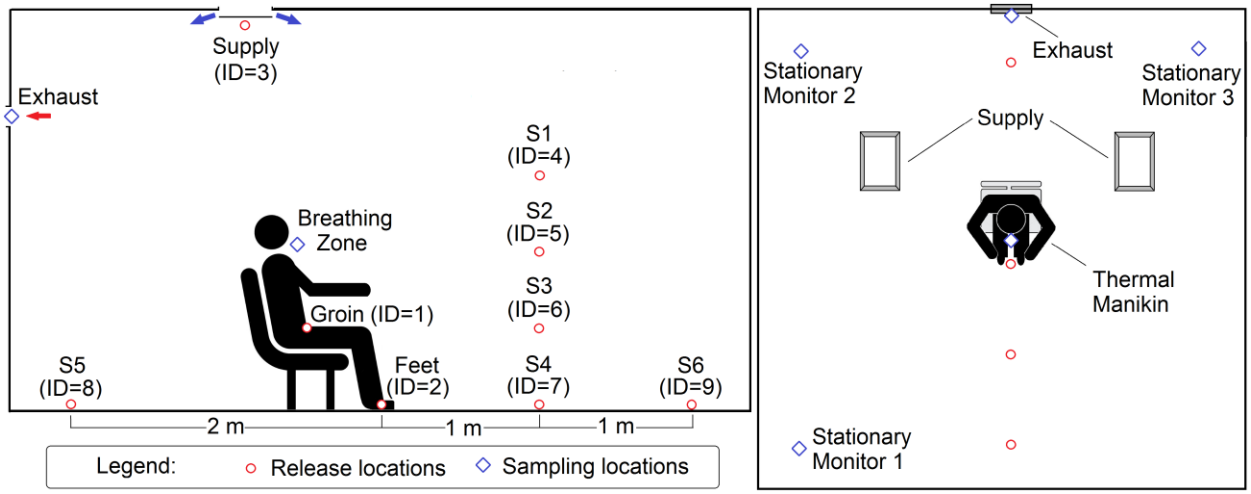


**Fig. 1.** Configuration of environmental chamber, including position of the manikin, source release and monitoring locations. The breathing zone personal monitor was positioned at 1.1 m height, and the exhaust monitor was placed at 1.8 m height. Stationary monitors 1, 2 and 3 were positioned at the three heights, 0.2, 1.1, and 1.7 m, respectively.

Experiments designed to investigate the inhalation intake fraction of PM released from human skin and clothing were performed with a human subject in the same experimental facility and under consistent environmental parameters (similar air-exchange rate, dry-bulb temperature and relative humidity). This part of the study utilized the measurement data from a related study [16] investigating the contributions of human envelope shedding to aerosol particle emissions indoors and to the personal cloud effect. We extend the analysis here by assessing the quantitative relationships between human PM emission rates and resultant inhalation intakes. During the experiments involving a human subject, the chamber was furnished with a table,

laptop computer and chair, all situated in the core of the experimental room. The male subject (1.85 m tall and 80 kg mass) followed a set of prescribed procedures prior to and during the experiments. The effects of PM release from the human envelope on the inhalation intake fractions were assessed for three activity types: sitting with moderate movement (simulated computer work, light stretching and combing hair), sitting with intensive movement (simulated exercising and manipulating imaginary papers and fabric), and walking at 80 steps/min (= 1 m/s). A detailed description of each activity type is presented in Table S1. Aided by the use of a metronome, each activity was executed at a constant pace and lasted for 30 minutes. Each source-active event in this study was followed by a post-release period of 1.5 h to allow monitoring of particle concentrations until they decayed to their background values.

### *2.3. Particle generation*

To experimentally quantify inhalation intake fractions in the deliberate injection experiments, it is essential to have an aerosol generation system that produces a consistent, quantifiable output of particles. A polydisperse aerosol was generated by means of a 6-jet Collison nebulizer (BGI Inc. Waltham, MA) using a solution of 10% olive oil in isopropyl alcohol (see schematic in Figure S1). Emissions were maintained at constant conditions for an interval of 10 minutes. The generated particles were released into the room through a stainless steel cylinder perforated on the upper side. The range of particle sizes that we focused on spanned diameters from 0.3 to 10 μm. These particles are respirable and typically include household dust and smoke, as well as the dominant size mode of airborne bacteria found indoors [26,27].

A performance test of the aerosol generation system ($n$ = 5) showed that it produced consistent emissions. The total $PM_{10}$ particle emission rate was 348 ± 23 mg/h. The coefficients

of variation (COV) for particles with diameters less than 7.5 µm varied 5-8%, while emissions of larger particles had a COV of 17%. Table S2 provides detailed methods and results for particle emissions characterization.

### *2.4. Instrumentation and sampling*

To assess the influence of several attributes on the source-receptor pathway, time- and size-resolved particle concentrations were monitored at multiple locations for both types of particle emissions (Figure 1): in the breathing zone as a proxy for personal exposure, in the exhaust vent to approximate room-average concentrations, and at three stationary locations to assess the degree of particle mixing throughout the room. The personal monitor was mounted on the subject's chest, with sampling inlet positioned within 0.15 m from the mouth.

To capture the effects of unsteady, dynamic processes and conditions, the particles were sampled with a time resolution of 1-min. The breathing zone and room-average levels were monitored with aerosol spectrometers (models 11-A and 1.108, GRIMM Aerosol Technik GmbH, Ainring, Germany). The particle number count was resolved in eight size bins based on optical diameter: 0.3-0.5 µm, 0.5-1 µm, 1-2 µm, 2-3 µm, 3-4 µm, 4-5 µm, 5-7.5 µm, 7.5-10 µm. Particle concentrations at the three stationary indoor locations were sampled and recorded by means of optical particle counters (model Met One HHPC 6+, Beckman Coulter Life Sciences, Palatine, IL, USA). Simultaneous indoor and outdoor $CO_2$ concentrations were monitored with time-resolved gas analyzers (LI-COR Biosciences, Lincoln, NE, USA). Dry-bulb temperature and relative humidity monitors were placed in the exhaust vent to sample and record the room-average values, as summarized in Table S3.

### 2.5. Data interpretation and intake fraction analysis

For particle number to mass conversion, we utilized a conversion algorithm that relies on three assumptions [28]: (a) particle density is 1 g/cm$^3$; (b) particles have a spherical shape; and (c) the mass-weighted size distribution is constant within each particle size bin. The estimated particle mass concentrations per size bin were summed to compute the $PM_{10}$ mass. The $PM_{10}$ mass included particles smaller than 10 µm and larger than 0.3 µm, which was the lower detection limit of our instruments. Particles below 0.3 µm were deemed to contribute negligibly to $PM_{10}$ in this study, based on expectations for mechanical generation of particulate matter.

The total inhalation intake fraction is defined as the ratio of the mass inhaled to the mass released from a source, as shown in equation (1). In this equation, it is assumed that: (a) exposure begins with the start of the emission event and finishes when particle concentration decays to the background value ($T \rightarrow \infty$); (b) the emission event occurs over a finite period, spanning from time 0 to time $T_\alpha$; and (c) only one person is exposed.

$$iF = \frac{M_{inh}}{M_{rel}} = \frac{Q_b \times \int_0^\infty C_{bz}(t)dt}{\int_0^{T_\alpha} E(t)dt} \quad (1)$$

In evaluating the intake fraction in this study, we assume that $Q_b$ = 0.5 m$^3$/h is the constant breathing flowrate for an individual at rest [29]. The parameter $C_{bz}(t)$ is the time-dependent particle concentration in the breathing zone; $E(t)$ is the time-dependent source emission rate. In applying equation (1) experimentally, the breathing zone concentration would be integrated from time 0 to a later time $T >> T_\alpha$, which is approximately the same as integrating to ∞ provided that the concentration resulting from the episodic emission has decayed to a negligible fraction of its peak value.

It is useful to decompose the intake fraction into three additive components representing exposure during three contiguous intervals [21]: the source-active period (the α period, spanning from time 0 to time $T_\alpha$); a transitional post-release period with non-uniform concentrations (the β period, from time $T_\alpha$ to time $T_\beta$); and the subsequent post-release period characterized by well-mixed concentrations above the background value (the γ period, from time $T_\beta$ to time $T_\gamma$). The total inhalation intake fraction is the sum of the three component values. Assuming that conditions remain unchanged from the previous equation, the total inhalation intake fraction becomes:

$$iF_i = \frac{Q_b \times \overline{C_{\iota,bz}(T)} \times T}{\overline{E_\iota(T_\alpha)} \times T_\alpha} = iF_i(T_\alpha) + iF_i(T_\beta) + iF_i(T_\gamma)$$

$$= \frac{Q_b}{\overline{E_\iota(T_\alpha)} \times T_\alpha} \times \left[\left(\overline{C_{\iota,bz}(T_\alpha)} \times T_\alpha\right) + \left(\overline{C_{\iota,bz}(T_\beta)} \times T_\beta\right) + \left(\overline{C_{\iota,bz}(T_\gamma)} \times T_\gamma\right)\right] \quad (2)$$

In applying equation 2 experimentally, we define the transition between the β and γ periods to occur when the COV of the $PM_{10}$ mass concentration detected by the three stationary monitors (Figure 1) declines to 10% of its maximum value [30]. For this set of chamber experiments, the duration of the β period varied with release duration, but only to a small degree (Figure S2). On average, the end of the β period occurred 12 min after the source-active period ($T_\beta$ = 12 min). The uncertainty in intake fraction evaluations associated with variable β duration was estimated to be low, within 6%. That estimate did not influence the results of the partial intake fraction during the source-active period $iF_i(T_\alpha)$, and the total intake fraction $iF_i$. In the experiments that involved a human subject, we only assessed exposures for the source-active or α period.

### 2.6. Source emission rate estimation

The experiments designed to investigate inhalation intake of the heated manikin and the human subject were performed under consistent ventilation rate, dry-bulb temperature and relative humidity. Differences in the two categories of experiments include: particle properties (olive oil vs. skin flakes, fragments and fibres); room air mixing (ventilation induced air mixing vs. a combination of ventilation and mixing induced by human motion); source release duration (10-min vs. 30-min) and furniture (only a chair for the manikin vs. presence of the table, chair and laptop for the human subject). For both emission types, the size-specific time-averaged source emission rate during the source-active period was computed based on a mass-balance model applied to the room-average particle number concentration recorded in the exhaust vent ($C_{i,room}$), as shown in equation (3):

$$\overline{E_i(T_\alpha)} = \frac{T}{T_\alpha} \times V\left[\frac{C_{i,room}(T) - C_{i,room}(0)}{T} + (a + k_i) \times \overline{C_{i,room}(T)}\right] \quad (3)$$

Here, the time $T_\alpha$ is the source-active period that spans from 0 to 10 min for the manikin experiments, and from 0 to 30 min for the human subject experiments; $V$ is the volume of the room; $a$ is the air exchange rate (1/h); and $k_i$ is the size-specific particle deposition loss-rate coefficient (1/h). For both experimental categories, the $k_i$ values were empirically estimated using the 1.5 h post-occupancy particle decay period in the experiments performed with a human subject. We assumed that the $k_i$ values obtained for the sitting activity are equal to the $k_i$ values for deliberate releases. (We lacked robust data to estimate the $k_i$ values directly from experiments involving the thermal manikin and controlled releases.) These $k_i$ values, presented in Table S4, agree reasonably with those reported by Thatcher et al. [31]. For equation (3), we assumed well-

mixed conditions. We also assumed negligible particle penetration from outdoors, as corroborated with very low background concentrations measured prior to each release event.

In experiments that involved the thermal manikin, we observed two trends associated with distinct particle fates: particles released near the floor (S4-S6) were largely removed from the air by means of gravitational settling onto the floor; whereas particles released at other locations were predominantly removed by ventilation. We interpret the evidence that particles released proximate to the floor were prone to enhanced gravitational settling because of the small distance between the source and the floor leading to short characteristic setting times for larger particles.

For the analyses reported for the manikin experiments in this manuscript, we adopted a constant source emission rate for each investigated release location, because the aerosol generation system produced a consistent output of particles (348 mg/h of $PM_{10}$). In experiments with the human subject, the emission rates differed for each activity type and were estimated based on measurements of particle concentrations at the ventilation outlet.

### *2.7. Quality assurance*

We anticipated that the results reported here were independent of the manikin's positioning with respect to the location of the air supply and exhaust vent. To assure that results are relevant to other indoor environments, separate tests were conducted with the manikin positioned at other location of the chamber and with the particles released near floor level. The intake fraction results agreed to within 5%, suggesting that the buoyant flows dominated over momentum driven flows in the breathing zone, and therefore that the results are not contingent on detailed airflow patterns induced by the ventilation system.

The $CO_2$ instrument response was confirmed through sampling of calibration gases at 0 and 1000 ppm. Data collected with calibrated stationary optical particle counters were corrected using adjustment factors from side-by-side tests of instrument performance (Table S5).

# 3. Results and Discussion

## *3.1. Intake fraction in a perfectly mixed environment*

As a baseline comparison, we utilized the modelling approach to estimate intake fraction in a perfectly mixed indoor environment. The calculation included both non-depositing and depositing particles. (In addition to removal by ventilation, particle loss by settling was taken into account for depositing particles.) Beyond the assumptions made in equations (1) and (2), we considered an ideal case in which the room air was instantaneously well mixed. As described in Nazaroff [1], the partial inhalation intake of non-depositing particles over the source-active period, $T \leq T_\alpha$, is given by this expression:

$$iF_i = \frac{Q_b}{Q}\left[\frac{T_\alpha}{T} - \frac{V}{QT}\left(1 - exp\left(-\frac{QT_\alpha}{V}\right)\right)\right] \quad (4)$$

The intake fraction for an exposure starting at the beginning of an emission event and extending beyond its completion (i.e., $T \geq T_\alpha$) is characterized by the following expression:

$$iF_i = \frac{Q_b}{Q}\left[1 - \frac{V}{QT_\alpha}\left(exp\left(\frac{QT_\alpha}{V}\right) - 1\right) \times exp\left(-\frac{QT}{V}\right)\right] \quad (5)$$

In equations (4) and (5), $Q$ is the room ventilation rate (= 115 $m^3$/h for the current experiments). To account for the size-specific particle deposition loss-rate coefficient (Table S4), equations (4) and (5) were amended by replacing each term $Q$ with $Q + k_iV$, representing a

change in which removal by ventilation becomes removal by the sum of ventilation plus deposition.

Table 1 reports predicted intake fraction results based on a well-mixed assumption for non-depositing and depositing particles. For this idealized case, the total intake fraction (for $T$ = 100 min, as an approximation to $T \rightarrow \infty$) for non-depositing particles would be 4.2‰. During the 10 min source-active period ($T_\alpha$), the partial intake fraction would be only 0.74‰, indicating that the post-release exposure period would dominate total inhalation intake for these conditions. Taking into account depositional loss mechanisms means that fewer airborne particles are available for inhalation exposure. The total predicted intake fraction would be reduced from 4.2‰ to 3.2‰, when incorporating the effects of depositional losses. This result is contingent on the size-specific particle emission rates reported in Table S2 and associated weighting factors reported in footnote b of Table 1.

**Table 1** Modelled inhalation intake fractions from episodic indoor releases in a well-mixed room for exposures spanning the duration of the source-active ($\alpha$) period (10 min) and for exposures spanning the full monitoring period (100 min). [a]

| **Source type** | **iF (‰) α period** | **iF (‰) full period** |
|---|---|---|
| Non-depositing particles in perfectly mixed environment | 0.74 | 4.2 |
| Depositing particles in perfectly mixed environment [b] | 0.70 | 3.2 |

[a] The release event began at $t$ = 0 and was continued for 10 min. The pollution was instantaneously mixed in the space ventilated with the volumetric flow rate of $Q$ = 115 $m^3$ $h^{-1}$ in a room of volume $V$ = 50 $m^3$. A single occupant was continuously exposed for indicated period from the beginning of release and inhaled at the breathing rate $Q_b$ = 0.5 $m^3$ $h^{-1}$. The α period and full period intake fractions were computed by using equations (4) and (5), respectively.
[b] For depositing particles, the estimates of the size-segregated intake fractions were combined into a single weighted-average intake fraction. The weighting factors, derived from the particle emission rates reported in Table S2, are the following: 0.3-0.5 µm: 0.05; 0.5-1 µm: 0.12; 1-2 µm: 0.17; 2-3 µm: 0.24; 3-4 µm: 0.18; 4-5 µm: 0.15; 5-7.5 µm: 0.08; 7.5-10 µm: 0.01. The size-specific particle deposition loss-rate coefficients ($k_i$) are from Table S4.

### *3.2. Empirical intake fractions: Impact of source location and exposure time*

Figure 2 shows measured inhalation intake fractions from nine localized source releases over the three integration periods for the experiments involving the thermal manikin. Overall, the

total intake fractions (for $T$ = 100 min, as an approximation to $T \to \infty$) ranged between 0.6 and 9.8‰ (600-9,800 ppm). Particles released proximate to the groin and feet of the manikin caused an inhalation intake over the full monitoring period of 9.8‰ and 6.6‰, respectively, which was comparable to the upper intake fraction limits reported in sleeping environments [18,19]. The inhalation intakes for other release locations (S1-S6) were smaller, ranging between 0.6‰ and 6.2‰. The finding of substantially higher material contribution to the inhalation intakes for releases proximate to the body is likely a combined effect of the proximity of the source to the manikin [32,33] and the influence of manikin's thermal plume transporting particles efficiently to the breathing zone [34-37].

Particles emitted at the room heights 0.5, 1 and 1.5 m (S1-S3) had higher inhalation intake fractions (4.4‰ to 6.2‰) compared to releases occurring near the floor (S4-S6, 0.6‰ to 1.6‰). Particles released near the floor were prone to enhanced loss rates owing to gravitational settling. Also noteworthy, the inhalation intake fraction for particles released at 1 m distance (S4, 1.6‰) was higher than when the release occurred at 2 m distance (S6, 0.6‰). These observations are qualitatively consistent with the understanding that source-receptor proximity, airflow patterns and particle attributes are each important factors that can influence the inhalation intake associated with episodic, localized sources.

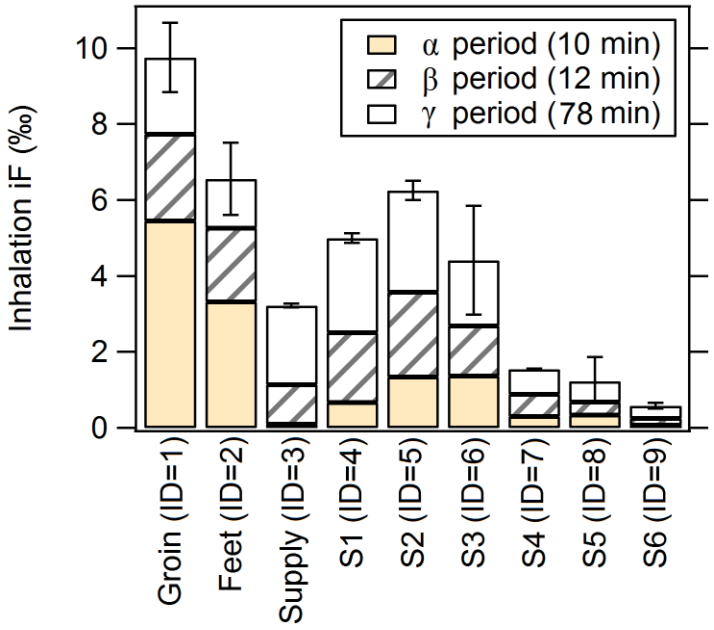


**Fig. 2.** Cumulative inhalation intake fraction for nine localized episodic indoor releases disaggregated into three exposure periods. For these experiments, the exposed subject was a seated, heated manikin.

Particles emitted at the supply air vent caused an inhalation intake fraction of 3.2‰. This empirical inhalation intake for the release at the supply vent was consistent with the theoretical inhalation intake of depositing particles under the well-mixed conditions, as reported in Table 1. The inhalation intake of particles emitted near the groin or the feet was higher than the inhalation intake recorded when the release occurred at the supply vent. This observation indicates that an individual particle with outdoor origin introduced into the room via mixing ventilation system is less likely to reach the breathing zone than a particle liberated near the envelope of a seated person. Furthermore, the particles introduced at the supply air vent had lower associated inhalation intake fractions compared to releases near the manikin at the room heights 0.5, 1 and 1.5 m (S1-S3).

Mage and Ott [21] have reported that if the well-mixed period ($T_\gamma$) is much longer than the sum of the release and unmixed periods ($T_\alpha + T_\beta$), then the well-mixed assumption may not

result in large errors in predicting exposures. Our findings indicate that this conclusion is contingent on particle release location. Even for long exposure periods, the well-mixed mass balance models could substantially underestimate inhalation intake when particle release occurs at certain indoor locations, in particular when releases occur near the exposed subject.

Furthermore, the well-mixed assumption might overestimate inhalation intake of coarse particles that are released at floor level away from a human, owing to efficient influence of gravitational settling across small heights in the absence of strong vertical mixing. On the other hand, comparing intake fractions when releases occurred in the supply vent and at the floor (S4) for particles smaller than 1 μm showed negligible difference. These smaller particles do not settle rapidly, so that the well-mixed model more suitably represents their behavior, as compared with supermicron particles.

Table 2 presents the quantitative contribution of three integration periods to the partial and total intake fractions for all examined indoor releases. The partial intake fractions during the source-active ($\alpha$) period ranged between 0.1‰ and 5.5‰. As seen both in Table 2 and in Figure 2, the partial intake fractions observed over the source-active phase exhibited much higher variability than did the full monitoring period. Particles released proximate to the groin and feet caused a partial inhalation intake for the $\alpha$ period of 5.5‰ and 3.3‰, respectively, which was much larger than $\alpha$-period intake fractions for particles released at various other locations, including the supply air vent (50×). This evidence supports a view that errors in exposure prediction could be larger during source-active periods than during full exposure periods that would include both source-active and post-release phases.

**Table 2** Summary of manikin experiments: mean ± standard deviation of inhalation intake fractions during the source-active (α = 10 min) period, unmixed (α + β = 22 min) period and the full monitoring period (α+β+γ = 100 min). [a, b]

| ID | Subject | Source | iF (‰) α period | iF (‰) α + β periods | iF (‰) full period |
|---|---|---|---|---|---|
| 1 | Manikin On | Groin | 5.5 ± 0.7 | 7.7 ± 0.8 | 9.8 ± 0.9 |
| 2 | Manikin On | Feet | 3.3 ± 0.5 | 5.3 ± 0.7 | 6.6 ± 0.9 |
| 3 | Manikin On | Supply | 0.1 ± 0.1 | 1.1 ± 0.1 | 3.2 ± 0.1 |
| 4 | Manikin On | S1 (1 m; 1.5 m height) | 0.7 ± 0.1 | 2.5 ± 0.2 | 5.0 ± 0.2 |
| 5 | Manikin On | S2 (1 m; 1 m height) | 1.3 ± 0.1 | 3.6 ± 0.2 | 6.2 ± 0.3 |
| 6 | Manikin On | S3 (1 m; 0.5 m height) | 1.4 ± 0.8 | 2.7 ± 1.1 | 4.4 ± 1.4 |
| 7 | Manikin On | S4 (1 m; 0.1 m height) | 0.3 ± 0.1 | 0.9 ± 0.1 | 1.6 ± 0.1 |
| 8 | Manikin On | S5 (2 m behind) | 0.3 ± 0.3 | 0.7 ± 0.4 | 1.2 ± 0.6 |
| 9 | Manikin On | S6 (2 m; 0.1 m height) | 0.1 ± 0.1 | 0.3 ± 0.1 | 0.6 ± 0.1 |
| 10 | Manikin Off | Groin | 0.05 | 0.1 ± 0.1 | 1.2 ± 0.2 |
| 11 | Manikin Off | Feet | 0.05 | 0.1 ± 0.1 | 0.7 ± 0.3 |

[a] For each experiment involving a thermal manikin, there were $n = 2$ replicates.
[b] Two supplementary experiments (ID = 10 and ID = 11) were conducted when the particles were released proximate to the groin and feet when there was no body heat (manikin was OFF) to investigate the effect of the thermal plume on the inhalation intake fraction of PM released from the manikin's body.

For episodic indoor releases occurring during occupied periods, exposure time often exceeds the source emission time. The inhalation intake fraction from such releases would continue to increase during the post-release period. As seen in Figure 2 and Table 2, for most of the studied locations, exposure is dominated by the post-release (β + γ) phase rather than the source-active (α) period. In these experiments, the contribution of the post-release period to total exposure ranged from 44% (ID=1) to 97% (ID=3). For particles released proximate to the manikin's groin and feet, the contributions to total inhalation intake were comparable during the source-active and post-release periods. For particles released at other indoor locations (S1-S6, Supply), the post-release period dominated the inhalation intake, contributing 69–97% of the total inhalation intake. Considering the nine experimental conditions with the manikin heated (ID=1 to 9), the 12-min unmixed transitional (β) period following the release event contributed 23–37% of the total intake fraction, without strong influence of release location.

Figure 3 illustrates the evolution of the partial inhalation intake fractions for nine localized indoor sources considering exposure periods in the range 0-100 minutes, referenced to the start of the particle release. The total interval includes the duration of the source-active (α) event (10 min), post-release unmixed (β) period (12 min), and post-release well-mixed (γ) period (up to 78 min). Particles emitted in the vicinity of the manikin produce a steeply rising inhalation intake during the source-release period. For the releases nearest to the manikin, the partial intake slopes diminish with time, indicating that rate of inhalation intake becomes smaller during the transitional β period and throughout the γ period. For particle releases at the other locations (S1-S6, Supply), the partial intake curves rise more slowly and steadily throughout the early portions of the exposure period. All curves exhibit diminishing slopes late in the exposure period as the emitted particles are lost from indoor air by a combination of ventilation and deposition. A relatively small variation among inhalation intakes during the well-mixed (γ) phase across all release locations is displayed in Figure S3. In summary, during the poorly mixed α and β periods, factors such as source location, proximity of the exposed person and airflow distribution patterns, are key variables influencing the inhalation intake. During the well-mixed γ stage, these factors become unimportant, and further contributions to intake depend mainly on factors that affect room-average concentrations, such as depositional and ventilation loss.

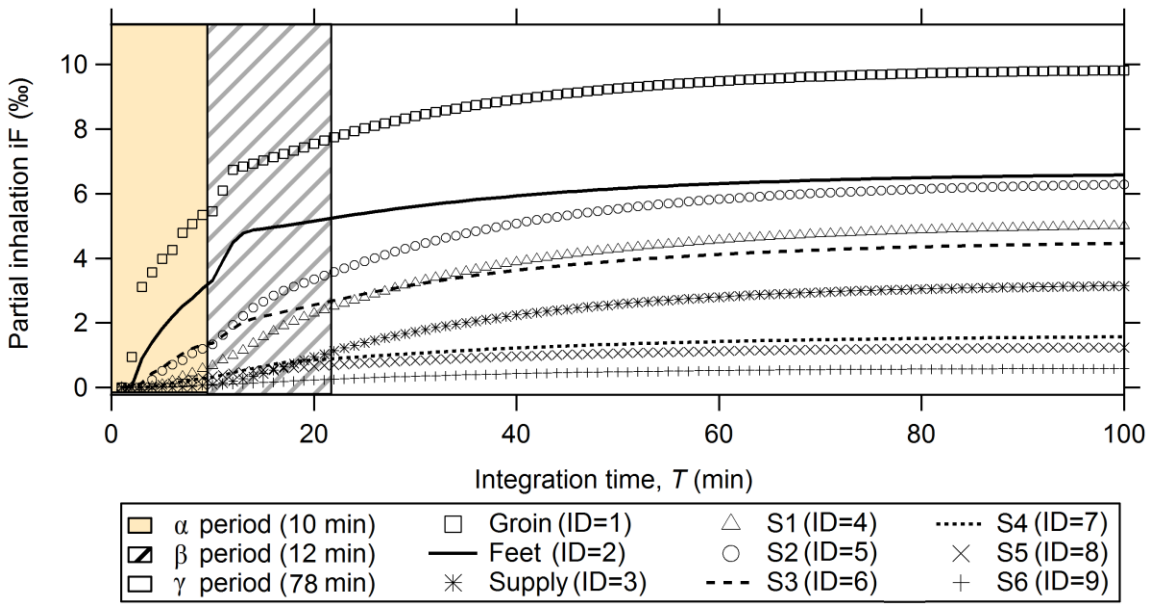


**Fig. 3.** Dynamic evolution of the partial inhalation intake fraction for nine localized episodic indoor release locations over the exposure period $T$ = 0 to 100 minutes.

### *3.3. Empirical intake fractions: Influence of the thermal plume*

To investigate the contribution of the buoyant thermal plume to inhalation intake, we conducted supplemental experiments with the particles released proximate to the groin (ID = 10) and feet (ID = 11), but with the manikin unpowered so that there was no associated thermal plume. For both release locations, the thermal plume strongly enhanced inhalation intake. As seen in Figure 4, the total inhalation intake of the heated manikin was 6.6‰ for releases near the feet (ID = 2), and 9.8‰ for releases near the groin (ID = 1). The corresponding inhalation intake fractions for the unheated manikin were almost an order of magnitude smaller (0.7‰ and 1.2‰, respectively). The substantial increase of inhalation intake for the heated manikin is attributed to the tendency of the thermal plume to draw particles upwards into the breathing zone. Results supporting this interpretation are also found in Licina et al. [37]. The results also indicate that the thermal plume can effectively enhance transport of particles in the size range 0.3-10 µm which are emitted

proximate to the human body. Conversely, in the absence of the thermal plume, particles larger than 1 μm are prone to enhanced gravitational settling (Figure 4). The influence of the thermal plume on inhalation intake may vary with various personal factors, such as the metabolic rate, type of activity, clothing and posture [36] and also with environmental factors, such as the room air temperature, ventilation rate and airflow distribution pattern [38].

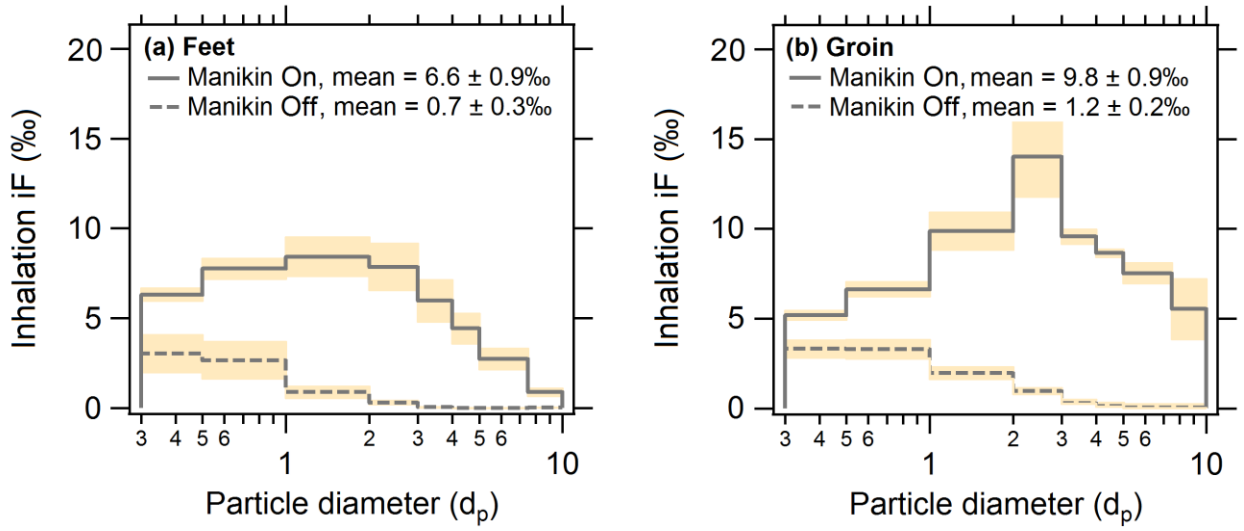


**Fig. 4.** Size-resolved inhalation intake fractions of deliberately released particles as a point source near (a) feet of a heated (ID = 2) and unheated manikin (ID = 11); and (b) groin of a heated (ID = 1) and unheated manikin (ID = 10). The mean ± standard deviation (illustrated by shaded area) across specified particle sizes are reported in both frames.

Experiments conducted with source locations proximate to the groin are intended to be indicative of coarse particle releases from the human skin and clothing. Similarly, source locations proximate to the feet are intended to represent particle resuspension from flooring and shoes while seated. These two mechanisms of occupant-associated coarse particle emissions contribute to the total aerosol mass indoors [13,16,39]. Humans are also a noteworthy indoor source of volatile organic compounds [40,41]. Clothing may be a source of airborne contaminants, e.g., from residual detergents [42] and post-manufacturing hazardous substances [43]. Ozone interactions with skin oils and personal care products may produce diminished

ozone concentrations but enhanced concentrations of reaction byproducts in the breathing zone [44,45]. Such pollutants could also have enhanced personal exposures owing to the thermal plume. Conversely, in spaces where the source of clean air is supplied near the floor level, the thermal plume can assist in transporting clean air into the breathing zone.

### *3.4. Empirical intake fractions for particle release from the human envelope*

Humans contribute materially to indoor coarse particle emissions [13]. We reinterpret here previously reported experimental data using a human subject in the same experimental room and under the same environmental conditions during 30-minute trials [16]. An aim was to characterize intake fractions associated with coarse particle generation from skin and clothing as influenced by normal occupant motions.

Figure 5 reports 30-min mean inhalation intake fractions in relation to PM emissions from the human envelope for three types of activities: seated with moderate movement (simulated computer work, light stretching and combing hair), seated with intensive movement (simulated exercising and manipulating imaginary papers and fabric) and walking at a constant pace of 80 steps/min (= 1 m/s) (see Table S1). The particle emission rates by mass (0.3-10 μm diameter range) as a consequence of these three activities are estimated based on equation (3) and also reported in Figure 5. In these experiments, exposures were assessed only for the 30-minute period that coincided with the generation activities. The reported inhalation intake fractions only consider exposures that occur during these 30-minute periods. The size-resolved inhalation intake fractions of particles released from the human subject are presented in Figure S4.

The three activity levels exhibit distinctive inhalation intake fraction values. For the sitting occupant performing moderate and intensive bodily movements, inhalation intake

fractions were 9.0‰ and 5.3‰, respectively. Remarkably, the walking subject had a significantly lower inhalation intake fraction at 0.9‰. The experimental data indicate, as one might expect, that the motion of the walking occupant contributes to more rapid mixing of the emitted particles throughout the room, whereas the thermal plume rising along the seated occupant contributes to spatial concentration gradients with elevated levels in the breathing zone.

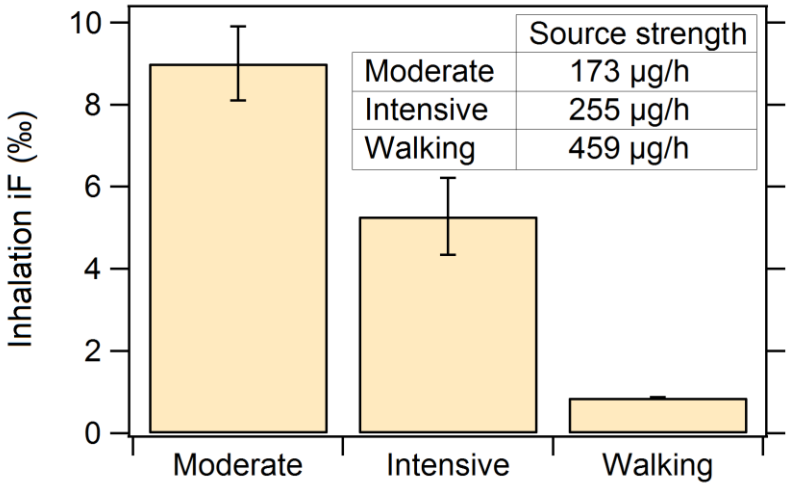


**Fig 5.** Inhalation intake fraction (mean ± standard deviation, *n*=3) during the 30-min mean source-active period as a result of three distinct occupant activities: seated with moderate movements, seated with intensive movements, and walking at 80 steps/min. The inset table indicates the human emission rates by mass for each activity, estimated based on equation (3). Note that the results reported here are valid for constant breathing flow rates ($Q_b$ = 0.5 $m^3$/h) across each activity type. We have also applied different breathing flow rates for three activities: $Q_b$ = 0.61 $m^3$/h for moderate activity, $Q_b$ = 1 $m^3$/h for intensive activity (these values are extrapolated from data reported by USA EPA [46]) and $Q_b$ = 0.84 $m^3$/h for walking at 1 m/s (extrapolated from data reported by Adams [29]). For these higher breathing rates, the inhalation intake fractions would be increased to 11‰ for moderate activity, 10.6‰ for intensive activity, and 1.4‰ for walking.

Although the walking person generated higher emission rates, the inhalation intake fraction while walking was considerably lower as compared to a seated person. Similarly, the seated occupant performing intensive bodily movements caused lower inhalation intake fraction relative to seated activity with moderate movement, despite higher emission rates. Overall, the intake fraction influence was more pronounced than the source strength effect, so that seated and

less vigorous activities were associated with higher inhalation intakes for the perihuman generation of coarse particles.

## 4. Conclusions

In a controlled environmental chamber with relatively clean surfaces and low background particle levels, we found that the source position, manikin thermal plume, and exposure duration considerably influence inhalation intake to episodically released particles from localized sources. With controlled releases, total inhalation intake fraction for particles (in the size range 0.3-10 μm) released from the human envelope averaged 7–10‰, considerably higher than for other indoor release locations. We found that these outcomes reflect the combined influence of the proximity of the source to the exposed subject and of the tendency of the thermal plume to transport particles from the lower perihuman environment to the breathing zone. The thermal plume alone contributed to substantially increased inhalation intake when the particles were released proximate to the groin or feet.

Relative to the well-mixed environment (intake fraction = 3.2‰ for experimental conditions of this study), the total inhalation intake increased up to 3× for particles released from the human envelope, and by 1.4–1.9× for nearby releases occurring at 0.5–1.5 m heights. These results suggest that the well-mixed representation of an indoor environment could underestimate the inhalation intake for certain types of indoor pollutant releases. A particular concern arises for emissions proximate to the body surface, which may more efficiently contribute to personal exposure than would particle emissions from other indoor locations. The risk of errors in exposure assessment is amplified during the poorly mixed source-active phase, relative to the post-emissions period.

Although exposure to emissions close the human envelope could be underestimated, we also found that the post-release and post-mixing period (i.e., the γ period) contributed substantially to total exposure. As established by prior research, that contribution is accurately estimated using the well-mixed room model. For the conditions studied here, with a release of 10-min duration and a post-release mixing time of 12 min at the beginning of a total exposure period of 100 min, and in a chamber with an air-exchange rate of 2.3 $h^{-1}$, the contribution to total exposure of well-mixed γ period was in the range 20–66%, depending on release location.

This is the first study to experimentally quantify inhalation intake fraction of particles released from the human skin and clothing. For coincident 30-min activity and exposure periods, inhalation intake varied primarily in relation to the human activity type, ranging from 0.9‰ for particles shed during walking to 9‰ for particles released during seated activities. Relative to walking, spatial concentration gradients were more pronounced when the occupant performed seated activities. Surprisingly, although particle emissions were stronger for walking and for vigorous seated activities, the inhalation intake — the product of the intake fraction and the cumulative emissions — was largest for the subject undertaking moderate activities while seated. This result reflects the very strong influence of the spatial concentration gradients affecting exposure for particles released from the human envelope. From a practical standpoint, in rooms that operate with low air mixing (e.g., with predominantly seated occupants), sensor positioning proximate to the human breathing zone may be key for accurately assessing inhalation intake.

The inhalation intake fraction metric is useful for elucidating source-receptor relationships, facilitating quantitative exposure evaluations, and supporting health risk assessments. The present study advances the understanding of how inhalation intake fraction varies in relation to spatially dependent episodic indoor emissions and influential transport

mechanisms, but has not considered variation in other building- and occupancy-related parameters and pollutant attributes. Further efforts are needed to probe the influences of different ventilation strategies, variable ventilation rates, higher occupancy levels and neutrally-buoyant pollution source. These efforts would be beneficial for assessing exposure conditions and associated health risks applicable in different types of indoor environments.

## Acknowledgements

Thanks are expressed to Dr. Randy Maddalena for arranging access to the environmental chamber at the Lawrence Berkeley National Laboratory and for technical assistance. The research was funded in part by a grant from the Alfred P. Sloan Foundation in support of the Berkeley Indoor Microbial Ecology Research Consortium (BIMERC). Additional support was provided by the Republic of Singapore's National Research Foundation through a grant to the Berkeley Education Alliance for Research in Singapore (BEARS) for the Singapore-Berkeley Building Efficiency and Sustainability in the Tropics (SinBerBEST) Program. BEARS has been established by the University of California, Berkeley as a center for intellectual excellence in research and education in Singapore.

## References

1. W.W. Nazaroff, Inhalation intake fraction of pollutants from episodic indoor emissions, Build. Environ. 43 (2008) 269–277.
2. D.H. Bennett, T.E. McKone, J.S. Evans, W.W. Nazaroff, M.D. Margni, O. Jolliet, et al., Defining intake fraction, Environ. Sci. Technol. 36 (2002) 206A–211A.
3. K.R. Smith, Air pollution: Assessing total exposure in the United States, Environment 30 (October 1988) 10–38.
4. A.C.K. Lai, T.L. Thatcher, W.W. Nazaroff, Inhalation transfer factors for air pollution health risk assessment, J. Air Waste Manage. Assoc. 50 (2000) 1688–1699.
5. W.W. Nazaroff, B.C. Singer, Inhalation of hazardous air pollutants from environmental tobacco smoke in US residences, J. Expo. Anal. Environ. Epidemiol. 14 (2004) S71–S77.
6. N.E. Klepeis, W.W. Nazaroff, Modeling residential exposure to secondhand tobacco smoke, Atmos. Environ. 40 (2006) 4393–4407.

7. L.A. Wallace, S.J. Emmerich, C. Howard-Reed, Source strengths of ultrafine and fine particles due to cooking with a gas stove, Environ. Sci. Technol. 38 (2004) 2304–2311.
8. G. Buonanno, L. Morawska, L. Stabile, Particle emission factors during cooking activities, Atmos. Environ. 43 (2009) 3235–3242.
9. C.M. Long, H.H. Suh, P. Koutrakis. Characterization of indoor particle sources using continuous mass and size monitors, J. Air Waste Manage. Assoc. 50 (2000) 1236–1250.
10. W.W. Nazaroff, C.J. Weschler, Cleaning products and air fresheners: Exposure to primary and secondary air pollutants, Atmos. Environ. 38 (2004) 2841–2865.
11. A.R. Ferro, R.J. Kopperud, L.M. Hildemann, Source strengths for indoor human activities that resuspend particulate matter, Environ. Sci. Technol. 38 (2004) 1759–1764.
12. R. Shaughnessy, H. Vu, Particle loadings and resuspension related to floor coverings in chamber and in occupied school environments, Atmos. Environ. 55 (2012) 515–524.
13. S. Bhangar, R.I. Adams, W. Pasut, J.A. Huffman, E.A. Arens, J.W. Taylor, et al., Chamber bioaerosol study: Human emissions of size-resolved fluorescent biological aerosol particles, Indoor Air 26 (2016) 193–206.
14. S. Bhangar, B. Brooks, B. Firek, D. Licina, X. Tang, M.J. Morowitz, et al., Pilot study of sources and concentrations of size-resolved airborne particles in a neonatal intensive care unit, Build. Environ. 106 (2016) 10–19.
15. D. Licina, S. Bhangar, B. Brooks, R. Baker, B. Firek, X. Tang, et al., Concentrations and sources of airborne particles in a neonatal intensive care unit, PLoS One 11 (2016) e0154991.
16. D. Licina, Y. Tian, W.W. Nazaroff, Emission rates and the personal cloud effect associated with particle release from the perihuman environment, Indoor Air (in press) doi: 10.1111/ina.12365.
17. N.E. Klepeis, Using computer simulation to explore multi-compartment effects and mitigation strategies for residential exposure to secondhand tobacco smoke, Ph.D. Dissertation, University of California, Berkeley, California, USA (2004).
18. M.P. Spilak, B.E. Boor, A. Novoselac, R.L. Corsi, Impact of bedding arrangements, pillows, and blankets on particle resuspension in the sleep microenvironment, Build. Environ. 81 (2014) 60–68.
19. B.E. Boor, M.P. Spilak, R.L. Corsi, A. Novoselac, Characterizing particle resuspension from mattresses: Chamber study, Indoor Air 25 (2015) 441–456.
20. J. Pantelic, K.W. Tham, D. Licina, Effectiveness of a personalized ventilation system in reducing personal exposure against directly released simulated cough droplets, Indoor Air 25 (2015) 683–693.
21. D.T. Mage, W.R. Ott, Accounting for nonuniform mixing and human exposure in indoor environments. In: B.A. Tichenor, ed., Characterizing sources of indoor air pollution and related sink effects. ASTM STP 1287 (1996) 263–278.
22. N.E. Klepeis, Validity of the uniform mixing assumption: Determining human exposure to environmental tobacco smoke, Environ. Health Perspect. 107 Suppl. 2 (1999) 357–363.
23. J.S. Russo, H.E. Khalifa, CFD assessment of intake fraction in the indoor environment, Build. Environ. 45 (2010) 1968–1975.
24. A. Melikov, J. Kaczmarczyk, Measurement and prediction of indoor air quality using a breathing thermal manikin, Indoor Air 17 (2007) 50–59.
25. D. Licina, A. Melikov, C. Sekhar, K.W. Tham, Air temperature investigation in microenvironment around a human body, Build. Environ. 92 (2015) 39–47.

26. J. Qian, D. Hospodsky, N. Yamamoto, W.W. Nazaroff, J. Peccia, Size-resolved emission rates of airborne bacteria and fungi in an occupied classroom. Indoor Air 22 (2012) 339–351.
27. D. Hospodsky, N. Yamamoto, W.W. Nazaroff, D. Miller, S. Gorthala, J. Peccia, Characterizing airborne fungal and bacterial concentrations and emission rates in six occupied children's classrooms, Indoor Air 25 (2015) 641–652.
28. J. Zhou, A. Chen, Q. Cao, B. Yang, V.W.C. Chang, W.W. Nazaroff, Particle exposure during the 2013 haze in Singapore: Importance of the built environment, Build. Environ. 93 (2015) 14–23.
29. W.C. Adams, Measurement of breathing rate and volume in routinely performed daily activities. Contract No. A033–205. Sacramento, CA, California Air Resources Board (1993).
30. A. Baughman, A.J. Gadgil, W.W. Nazaroff, Mixing of a point source pollutant by natural convection flow within a room, Indoor Air 4 (1994) 114–122.
31. T.L. Thatcher, A.C.K. Lai, R. Moreno-Jackson, R.G. Sextro, W.W. Nazaroff, Effects of room furnishings and air speed on particle deposition rates indoors, Atmos. Environ. 36 (2002) 1811–1819.
32. S.J. McBride, A.R. Ferro, W.R. Ott, P. Switzer, L.M. Hildemann, Investigations of the proximity effect for pollutants in the indoor environment, J. Expo. Anal. Environ. Epidemiol. 9 (1999) 602–621.
33. V. Acevedo-Bolton, W.R. Ott, K.C. Cheng, R.T. Jiang, N.E. Klepeis, L.M. Hildemann, Controlled experiments measuring personal exposure to $PM_{2.5}$ in close proximity to cigarette smoking, Indoor Air 24 (2014) 199–212.
34. H. Brohus, P.V. Nielsen, Personal exposure in displacement ventilated rooms, Indoor Air 6 (1996) 157–167.
35. M. Salmanzadeh, Gh. Zahedi, G. Ahmadi, D.R. Marr, M. Glauser, Computational modeling of effects of thermal plume adjacent to the body on the indoor airflow and particle transport, J. Aerosol Sci. 53 (2012) 29–39.
36. D. Licina, J. Pantelic, A. Melikov, C. Sekhar, K.W. Tham, Experimental investigation of the human convective boundary layer in a quiescent indoor environment, Build. Environ. 75 (2014) 79–91.
37. D. Licina, A. Melikov, J. Pantelic, C. Sekhar, K.W. Tham, Human convection flow in spaces with and without ventilation: Personal exposure to floor-released particles and cough-released droplets, Indoor Air 25 (2015) 672–682.
38. D. Licina, A. Melikov, C. Sekhar, K.W. Tham, Human convective boundary layer and its interaction with room ventilation flow, Indoor Air 25 (2015) 21–35.
39. R.I. Adams, S. Bhangar, W. Pasut, E.A. Arens, J.W. Taylor, S.E. Lindow, et al., Chamber bioaerosol study: Outdoor air and human occupants as sources of indoor airborne microbes, PLoS One 10 (2015) e0128022.
40. S. Liu, R. Li, R.J. Wild, C. Warneke, J.A. de Gouw, S.S. Brown, et al., Contribution of human-related sources to indoor volatile organic compounds in a university classroom, Indoor Air 26 (2016) 925–938.
41. X. Tang, P.K. Misztal, W.W. Nazaroff, A.H. Goldstein, Volatile organic compound emissions from humans indoors, Environ. Sci. Technol. 50 (2016) 12686–12694.
42. T. Kiriyama, H. Sugiura, M. Uehara, Residual washing detergent in cotton clothes: A factor of winter deterioration of dry skin in atopic dermatitis, J. Dermatol. 30 (2003) 708–712.
43. G. Luongo, G. Thorsén, C. Östman, Quinolines in clothing textiles — A source of human exposure and wastewater pollution? Anal. Bioanal. Chem. 406 (2014) 2747–2756.

44. R.L. Corsi, J. Siegel, A. Karamalegos, H. Simon, G.C. Morrison, Personal reactive clouds: Introducing the concept of near-head chemistry, Atmos. Environ. 41 (2007) 3161–3165.
45. D. Rim, A. Novoselac, G. Morrison, The influence of chemical interactions at the human surface on breathing zone levels of reactants and products, Indoor Air 19 (2009) 324-334.
46. U.S. Environmental Protection Agency, Metabolically derived human ventilation rates: A revised approach based upon oxygen consumption rates, Report EPA/600/R-06/129F, Washington, DC (2009).

## Appendix A. Supplementary data

**Table S1.** Detailed description of the human activity type and duration.

**Table S2.** Average particle mass emission rates (mean ± standard deviation) obtained with the aerosol generation system ($n$ = 5).

**Table S3.** The room-average values (time-averaged mean) of the dry-bulb temperature and relative humidity for each experimental run.

**Table S4.** Comparison between empirically derived, size-resolved deposition loss rate coefficients (mean ± standard deviation, $n$ = 3, units = $h^{-1}$) for sitting and walking activity and values from Thatcher et al. [1].

**Table S5.** Adjustment factors derived for optical particle counters (OPCs, model GRIMM) and stationary monitors (SM, model Met One) from side-by-side tests with reference instruments $OPC_1$ and $SM_3$.

**Fig. S1.** Schematic of the particle generation system that consisted of compressed air, valve, HEPA filter, pressure gauge, 6-jet Collison nebulizer (18.55 PSA, 3.5 LPM), three dilution branches with HEPA filters and a stainless-steel single-ended cylinder perforated on the upper side to allow particle discharge.

**Fig. S2.** Time-resolved coefficient of variation of the $PM_{10}$ mass among three stationary monitors for various release locations.

**Fig. S3.** Time-resolved coefficient of variation of the partial inhalation intake fraction averaged across nine experiments, with different source locations (ID = 1 to 9).

**Fig. S4.** Size-resolved partial inhalation intake fractions of particles naturally released from the sitting human via (a) moderate and (b) intensive sitting activities and (c) from the walking human.

**Figure 1**

Click here to download high resolution image

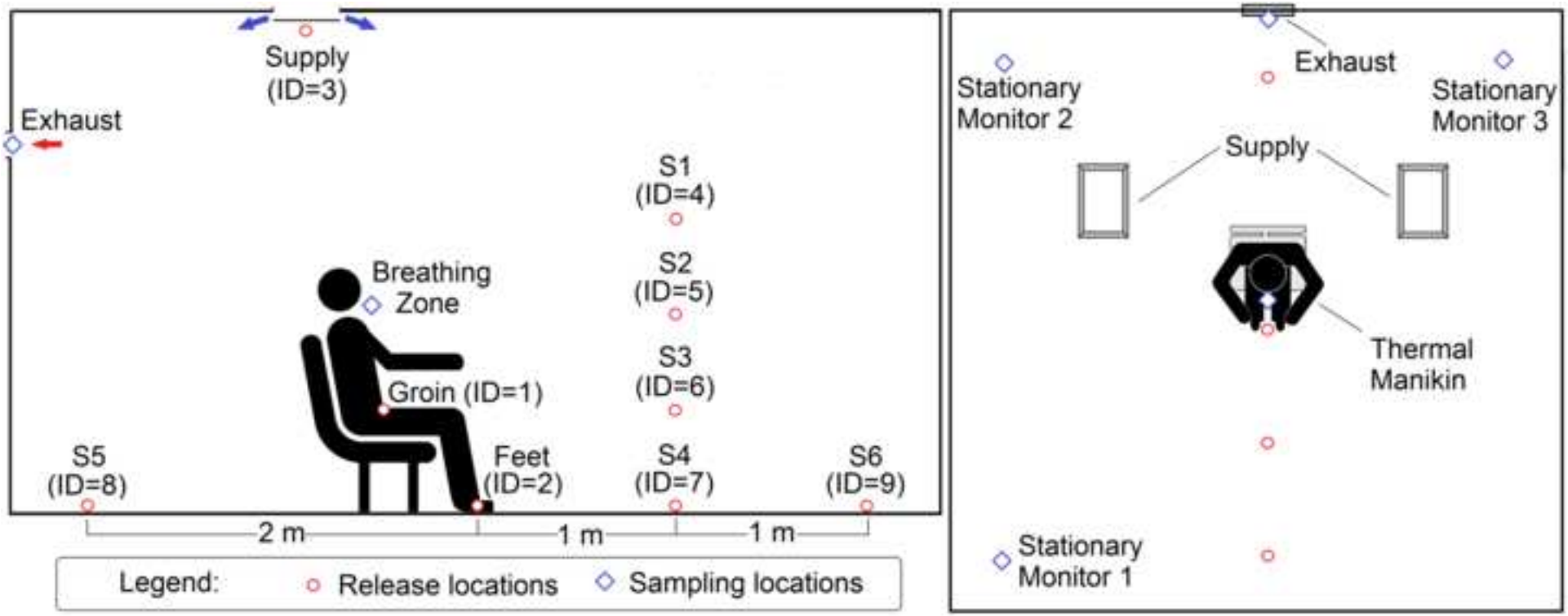

**Figure 2**

Click here to download high resolution image

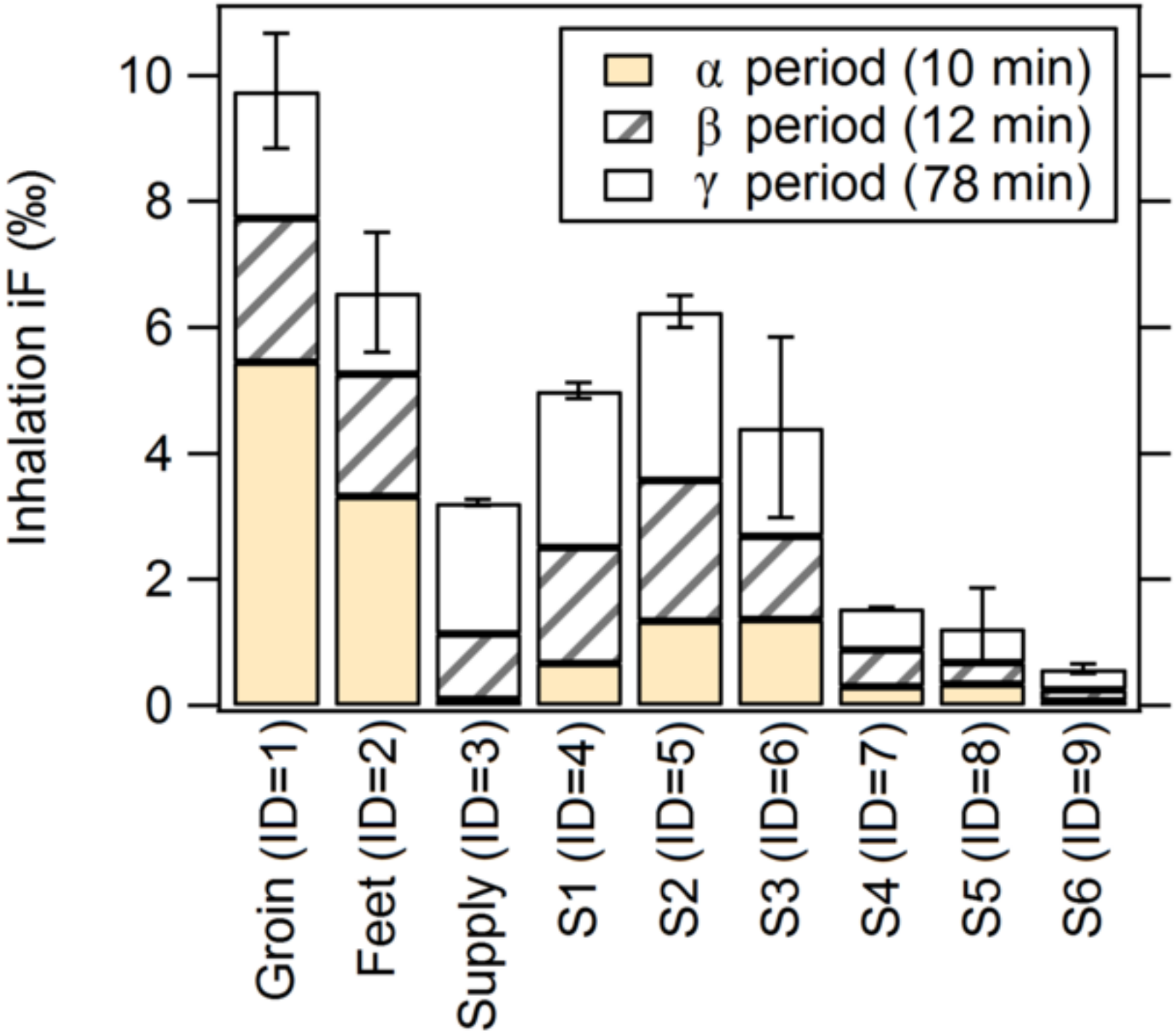

**Figure 3**

Click here to download high resolution image

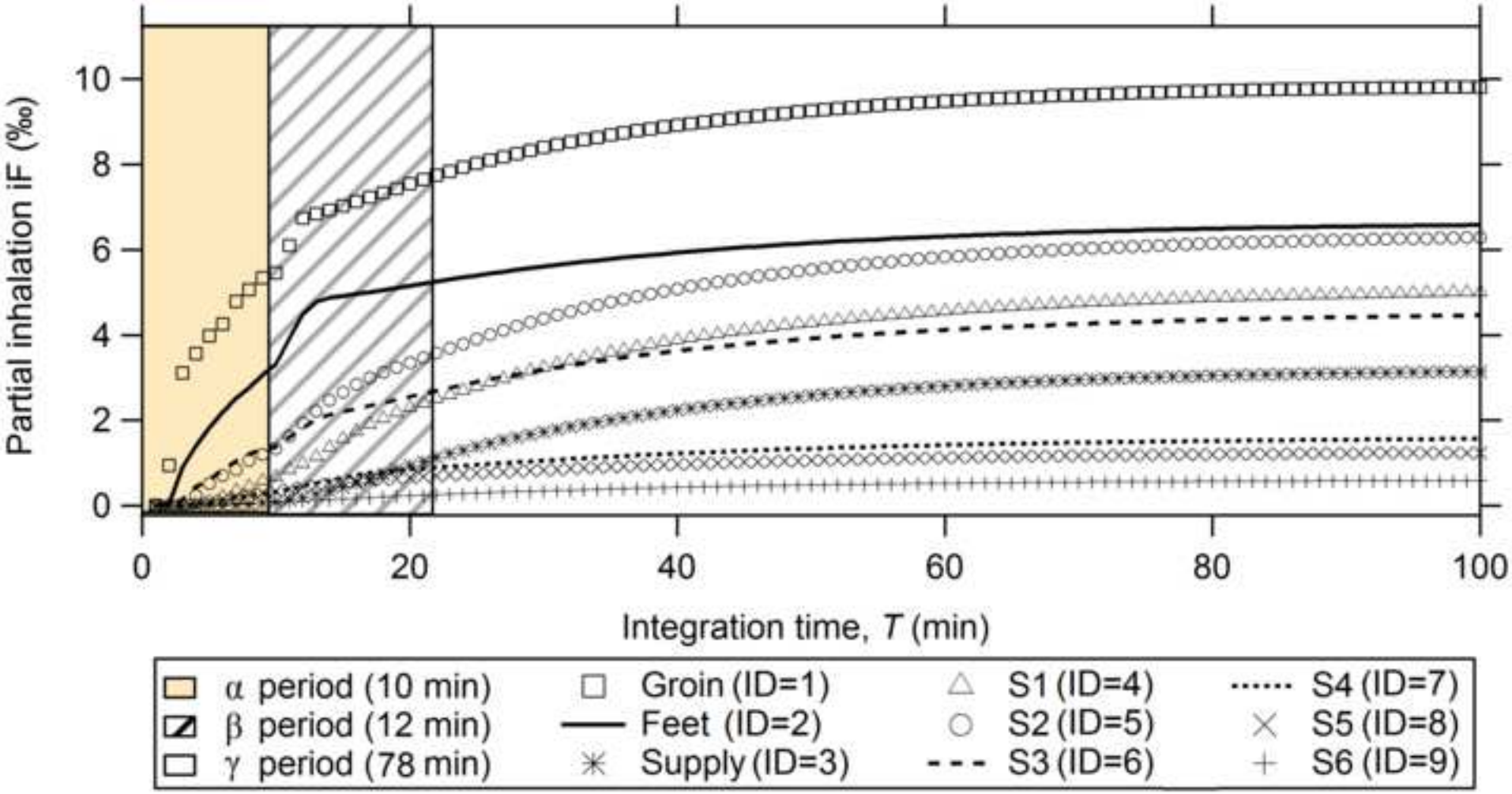

Figure 4

Click here to download high resolution image

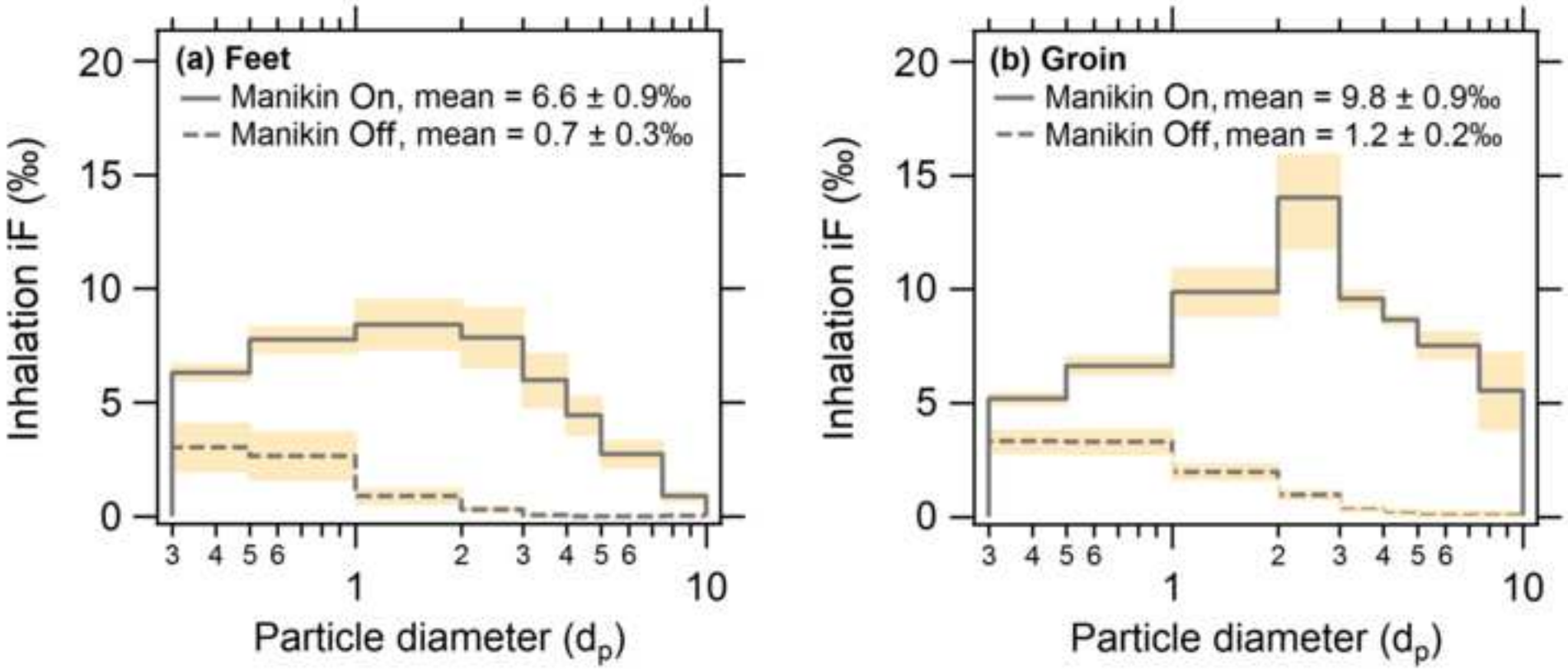

Figure 5

Click here to download high resolution image

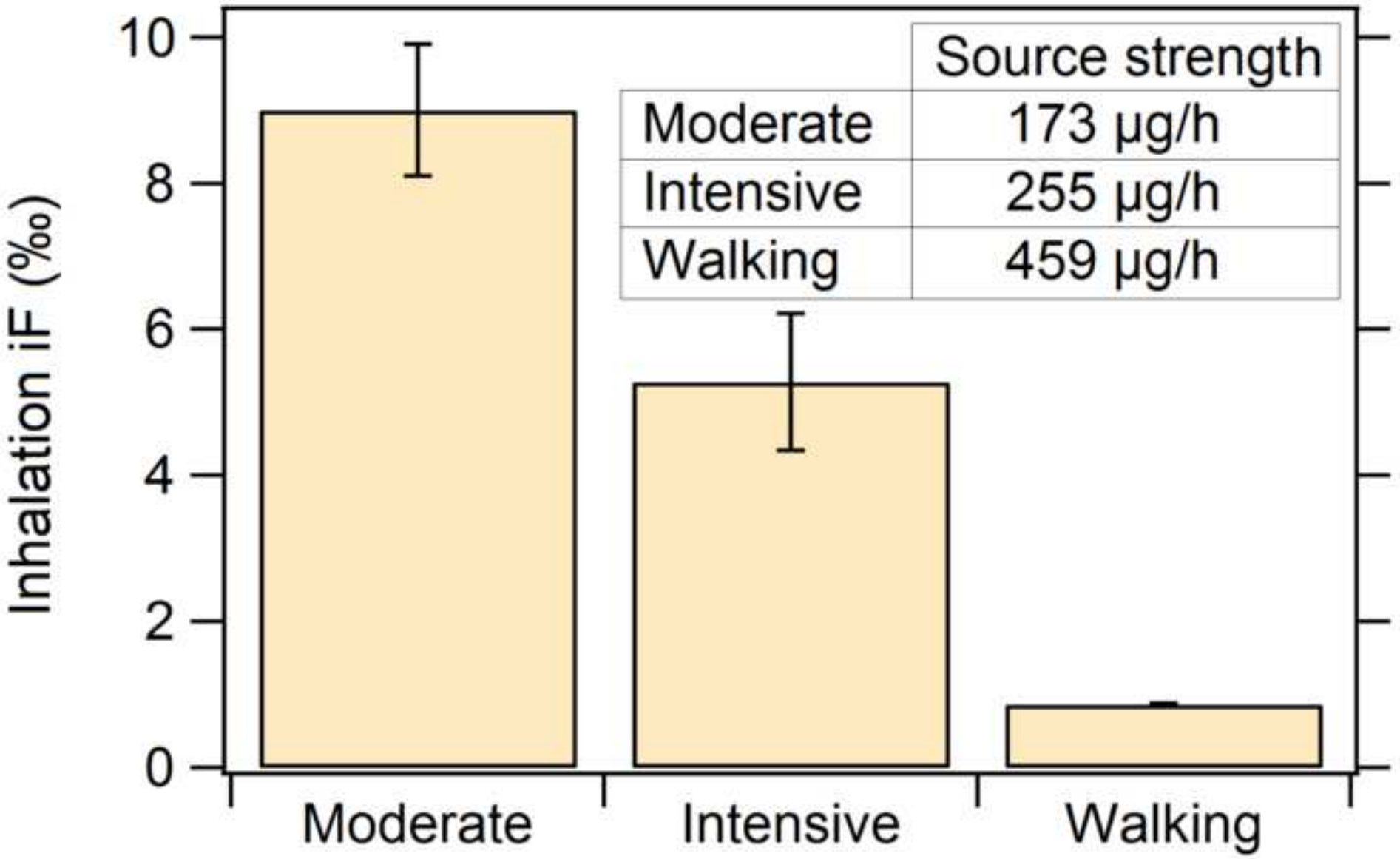

**Supporting information**

**Click here to download e-component: Licina et al BAE_supporting information.docx**

**Figure S1**

**Click here to download e-component: Figure S1.png**

**Figure S2**

**Click here to download e-component: Figure S2.png**

**Figure S3**

**Click here to download e-component: Figure S3.png**

**Figure S4**

**Click here to download e-component: Figure S4.png**